Letter

Achieving Robust Single-Photon Blockade with a Single Nanotip

Jian Tang, Yunlan Zuo, Xun-Wei Xu, Ran Huang,* Adam Miranowicz, Franco Nori, and Hui Jing*

Cite This: *Nano Lett.* 2025, 25, 4705−4712

Read Online

ACCESS | 📊 Metrics & More | 📰 Article Recommendations

ABSTRACT: Backscattering losses (BSL), arising from intrinsic imperfections or unavoidable external perturbations in optical resonators, can severely impact photonic devices. In single-photon systems, robust quantum correlations against BSL remain largely unexplored despite their significance for various applications. Here, we demonstrate that single-photon blockade (SPB), a purely quantum effect, can be preserved against BSL by introducing a nanotip near a Kerr nonlinear resonator with intrinsic defects. Without the tip, BSL disrupts SPB, but tuning the tip's position restores robustness even under strong BSL. Notably, quantum correlations emerge while the classical mean photon number remains suppressed due to the interplay between resonator nonlinearity and tip-induced optical coupling. Our findings highlight nanoscale engineering as a powerful tool to protect and harness fragile quantum correlations, paving the way for robust single-photon sources and backscattering-immune quantum devices.

KEYWORDS: *backscattering loss, photon blockade, nanotip, quantum correlation, single photon, optical nonlinearity*
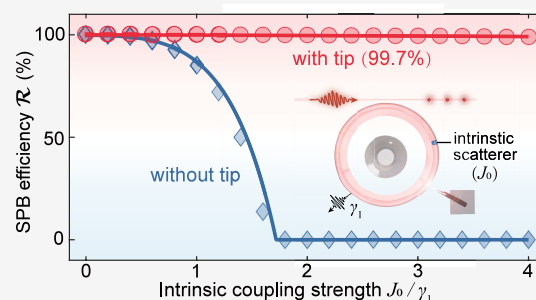
Single-photon quantum optics is pivotal for advancing quantum information technologies, enabling applications such as quantum communications,[1−3] quantum computing,[4−7] and quantum optical metrology.[8] In this context, single-photon blockade (SPB),[9−12] indicating blockade of the subsequent photons by absorbing the first one, goes beyond classical optics and laser physics into a purely quantum regime. Due to its crucial role in generating nonclassical correlations and constructing single-photon devices, SPB has been demonstrated experimentally in various systems ranging from micro- or nanoscale cavities with atoms,[13−15] quantum dots,[16−20] or superconducting qubits,[21−25] to cavity-free atoms[26,27] or Bose-Hubbard chains.[28] In addition, multiphoton blockade[29−31] has recently been observed, opening the way to create few-photon devices for quantum networks.

Optical whispering-gallery-mode (WGM) microresonators are excellent platforms for achieving SPB due to their ability to confine light in a circular path within a microscale volume, leading to strongly enhanced light-matter interactions. These microresonators are not only significant for fundamental studies in nonlinear optics[32,33] but also play a crucial role in nano-optics applications, particularly ultrasensitive nanoscale sensing.[34−38] However, In a real WGM cavity, imperfections—like intrinsic material defects, density variations, or surface roughness—can cause backscattered light in the counter-propagating direction, leading to an extra optical loss and mode coupling. Such backscattering has been used to realize counter-propagating solitons,[39] chiral lasing,[40] absorption[41] and topological,[42] as well as slow light and its localization.[43] However, backscattering loss limits the application perform-

ance in classical and quantum devices, such as instability problems in frequency combs,[44,45] backscattering-induced noise, and lock-in effect in optical gyroscopes,[46−48] as well as decrease of secure key rates in quantum key distribution.[49,50]

To overcome these challenges, backscattering loss suppression was experimentally studied by introducing reflectors or scatterers, ranging from macroscale mirrors[51,52] to Mie[53] and Rayleigh[54] scatterers. Also, Brillouin scattering,[55,56] active feedback control,[57] self-injection technique,[58] and synthetic gauge fields[59] were used to suppress backscattering. These remarkable achievements provide powerful tools to optimize optical devices[56] and explore nonreciprocal optics[59] or non-Hermitian physics.[60] Yet previous efforts have been devoted to propagation against backscattering loss of *many photons or classical light*,[51−57,59−62] it is essential to study robust nonclassical single-photon effects in spite of intrinsic defects, which are expected to play a key role in realistic single-photon devices and quantum technologies.
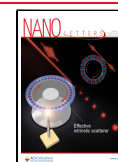
In this letter, we study the realization of *robust quantum correlation of single photons* against backscattering loss via the SPB effect in nonlinear WGM cavities by introducing a nanotip. Although, backscattering loss can lead to the breakdown of SPB in conventional WGM cavities, we find
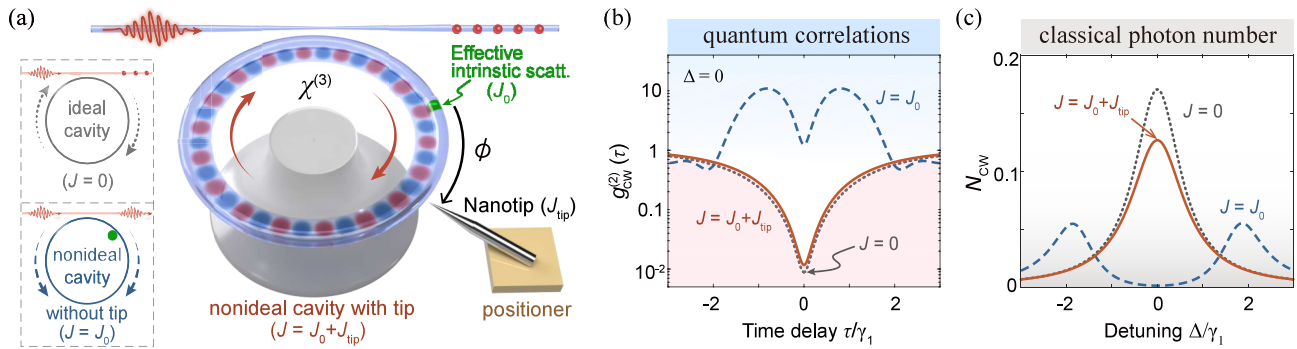
Figure 1. SPB against backscattering loss in a Kerr WGM cavity with an additional tip. (a) SPB occurs in an ideal nonlinear cavity (gray, $J = 0$), and is annihilated by the backscattering in a nonideal cavity (blue, $J = J_0$). SPB reoccurs by tuning the relative distance ϕ between the intrinsic scatterer (J_0) and the tip (J_{tip}). (b) These effects are confirmed via the quantum correlation $g_{cw}^{(2)}(\tau)$. (c) Mean photon number N_{cw} versus Δ/γ_1. Here, $J_0 = 1.8\gamma_1 \sim 0.4$ MHz, $\chi/\gamma \sim 5.3$, $\phi = 0.27$ μm. The other parameters are given in the main text.

robust SPB can be revived with an efficiency of up to 99.7% by precisely tuning the position of the nanotip, and it is robust with different backscattering strengths. Different from the behavior of classical mean photon number, SPB can emerge when the mean photon number is still suppressed, since our findings do not merely rely on the nanotip-induced destructive interference,[51−54] but on the *interplay* of the resonator nonlinearity and the nanotip-induced optical coupling. Instead of analyzing light amplitudes,[51−57,59,60] we focus on quantum correlations and the transitions between quantum states, which hold the potential for implementations in quantum information technologies. Our findings drive the field of backscattering suppression into the quantum regime, hence making it possible to realize a variety of quantum backscattering-immune effects, such as multiphoton blockade against backscattering loss[29−31] or one-way single-photon transmission,[63,64] for potential applications of nanoscale engineering in robust quantum devices and the protection of fragile quantum resources.

We consider an optical Kerr resonator with an additional nanotip [Figure 1(a)]. For an ideal cavity driven from the left-hand side, only the clockwise (CW) mode is dominant. In a real cavity, intrinsic defects cause backscattering in the counterclockwise (CCW) direction, which can be approximated as an effective single scatterer,[54,65] leading to the coupling between the CW and CCW modes (with strength J_0).[66−68] We note that the intrinsic backscattering strength is proportional to J_0.[69−71] Introducing a nanotip also leads to coupling between the two modes, which can in general be nonsymmetric leading to the studies of non-Hermitian physics with exceptional points.[53,66,72−74] However, such couplings are typically assumed to be equal (i.e., without exceptional points).[41,75,76] Thus, the total optical coupling can be written as ($\hbar = 1$):

$$\hat{H}_j = J\hat{a}_1^\dagger \hat{a}_2 + J^* \hat{a}_2^\dagger \hat{a}_1, \quad J = J_0 + J_{tip},$$
$$J_{tip} = a_t \exp(-2\beta_t r)\exp(-i\Theta) \tag{1}$$

Here, $\hat{a}_1$ ($\hat{a}_2$) is the annihilation operator for the CW (CCW) mode, J_{tip} is the tip-induced coupling strength with amplitude a_t, decay coefficient β_t, and radial distance r. The relative phase of the effective intrinsic scatterer and the tip is $\Theta = 2k_{opt}\phi + \theta + \theta_t r$, where ϕ is the relative azimuthal distance, $k_{opt} = 2\pi n_0/\lambda$ is the optical wavenumber with refractive index n_0 and vacuum wavelength of light λ, θ is the initial phase, and θ_t is a radially dependent phase accounting for the tip shape.[54]

To study SPB against backscattering loss, we consider a generic nonlinearity, Kerr nonlinearity,[10,12,77] which was realized via light-atom couplings,[13,78] superconducting circuits,[79] and magnon devices,[80] as well as theoretically studied in optomechanical systems.[81−84] The Kerr interactions are given by[85−88]

$$\hat{H}_k = \sum_{j=1,2} \chi \hat{a}_j^\dagger \hat{a}_j^\dagger \hat{a}_j \hat{a}_j + 2\chi \hat{a}_1^\dagger \hat{a}_1 \hat{a}_2^\dagger \hat{a}_2 \tag{2}$$

where $\chi = 3(\hbar\omega)^2 \overline{\chi}^{(3)}/(4\varepsilon_0 \overline{\varepsilon_r}^2 V_{eff})$ is the Kerr parameter with nonlinear susceptibility $\overline{\chi}^{(3)}$, vacuum (relative) permittivity ε_0 ($\overline{\varepsilon_r}$), and mode volume V_{eff}.[85,86,89−91] In this work, We adopt a scalar approximation for $\overline{\chi}^{(3)}$ to estimate results at the order-of-magnitude level, neglecting the off-diagonal components of $\chi_{ijkl}^{(3)}$ to simplify the analysis.[89,91,92] Such Kerr interaction becomes $\hat{H}_k = \chi \hat{a}_1^\dagger \hat{a}_1^\dagger \hat{a}_1 \hat{a}_1$ in an ideal cavity. In the frame rotating at the drive frequency ω_L, the Hamiltonian of the system reads

$$\hat{H}_r = \Delta(\hat{a}_1^\dagger \hat{a}_1 + \hat{a}_2^\dagger \hat{a}_2) + \hat{H}_j + \hat{H}_k + \xi(\hat{a}_1^\dagger + \hat{a}_1) \tag{3}$$

with $\Delta = \omega - \omega_L$, and $\omega = \omega_0 + |J|$. Here, ω_0 is the resonance frequency of the cavity, $\xi = [\gamma_{ex}P_{in}/(\hbar\omega_L)]^{1/2}$ is the driving amplitude with power P_{in} and cavity-waveguide coupling rate γ_{ex}.

We study the classical mean photon number $N_{cw} = \langle \hat{a}_1^\dagger \hat{a}_1 \rangle$, and the second-order quantum correlation:[93] $g_{cw}^{(2)}(\tau) \equiv \lim_{t \to \infty} [\langle \hat{a}_1^\dagger(t)\hat{a}_1^\dagger(t+\tau)\hat{a}_1(t+\tau)\hat{a}_1(t)\rangle / \langle \hat{a}_1^\dagger(t)\hat{a}_1(t)\rangle^2]$, which is usually measured by Hanbury Brown-Twiss interferometers.[13−17] The condition $g_{cw}^{(2)}(0) < g_{cw}^{(2)}(\tau)$ characterizes photon antibunching, and $g_{cw}^{(2)}(0) \ll 1$ [or $g_{cw}^{(2)}(0) \approx 0$] indicating SPB with sub-Poissonian photon-number statistics.[12,13,94,95]

This $g_{cw}^{(2)}(\tau)$ can be calculated by numerically solving the Lindblad master equation for the density operator $\hat{\rho}$ of this system:[96,97]

$$\dot{\hat{\rho}} = -i[\hat{H}_r, \hat{\rho}] + \sum_{j=1,2} \frac{\gamma}{2}(2\hat{a}_j\hat{\rho}\hat{a}_j^\dagger - \hat{a}_j^\dagger \hat{a}_j \hat{\rho} - \hat{\rho}\hat{a}_j^\dagger \hat{a}_j) \tag{4}$$

where $\gamma = \gamma_1 + \gamma_{tip}$ is the total dissipation rate, $\gamma_1 = \gamma_0 + \gamma_{ex}$, and $\gamma_0 = \omega_0/Q$ denotes the intrinsic losses of the cavity with the quality factor Q. The tip-induced loss is $\gamma_{tip} = a_\gamma\exp(-2\beta_\gamma r)$, with amplitude a_γ, and decay coefficient β_γ.[54]

The experimentally accessible parameters of the nanotip are taken as[54] $a_t = 14.3$ MHz, $(2\beta_t)^{-1} = 99$ nm, $\theta_t = 3\pi/2$ μm^{-1}, $\theta = -\pi/2$, $a_\gamma = 2.43$ MHz, and $(2\beta_\gamma)^{-1} = 92$ nm. The other experimentally accessible parameters are[87,88,98−101] $V_{eff} = 150$

μm^3, $n_0 = 1.4$, $Q = 10^{10}$, $\lambda = 1550$ nm, $\chi^{(3)}/\varepsilon_r^2 = 1.8 \times 10^{-17}$ m^2/V^2, and $P_{in} = 4$ fW. For the WGM cavities, V_{eff} is typically $10^2 - 10^4\ \mu m^3$,[98,99] $Q \sim 10^9 - 10^{12}$,[100,101] and $J_0 \sim 0.5$ MHz-0.1 GHz.[55,56,102,103] The Kerr coefficient for semiconductor materials with GaAs is $\chi^{(3)}/\varepsilon_r^2 = 2 \times 10^{-17}$ m^2/V^2,[87,88] and materials with indium tin oxide reach $\chi^{(3)}/\varepsilon_r^2 = 2.12 \times 10^{-17}$ m^2/V^2.[104] In addition, $\chi^{(3)}$ can be further enhanced to 2×10^{-11} m/V^2 with other materials.[89,105] The input power can be attenuated by passing through an electro-optic modulator, and reach to 6.3 fW.[106] Since $P_{in} \ll \gamma$, the thermal effect induced by high optical powers can be neglected.[107] Thermal effects can also be reduced by making a thermal isolation or changing the materials of the bracket to, for instance, aluminum.[108] In experiments, the nanotip can be fabricated on a high-purity polycrystalline tungsten wire with an electrochemical etching process, which relies on capillary action and water-based electrochemical reactions.[107] The tip size can be precisely controlled by adjusting the etching-voltage cutoff delay. Additionally, the tungsten tip near-field probe is fixed onto a polylactic acid plastic mount, which is then attached to a computer-controlled, three-axis piezoelectric positioner. This setup allows for a positioning precision of 25 nm or even smaller.[107] Also, realistic mechanical instability or temperature drift can be eliminated by designing a chip-based resonator with a scatterer integrated on the chip,[109] which holds the potential for realizing backscattering-immune on-chip resonators based on microelectromechanical-systems (MEMS) techniques.

Figure 1(b) shows SPB with $g_{cw}^{(2)}(0) \sim 0.009$ in an ideal Kerr cavity, since the input light fulfilling the single-photon resonance condition ($\Delta = 0$) can only be resonant with the transition from the vacuum to the one-photon state but not with higher transitions.[12,13] However, intrinsic defects in a nonideal cavity cause backscattering and a coupling J_0 [the mode splitting in Figure 1(c)], which provides an extra path for the resonance of higher-state transitions, leading to the breakdown of SPB.

In contrast, SPB recovers with a tip [Figure 1(b)], which is also confirmed by higher-order correlations: $g_{cw}^{(4)}(0) \sim 4.8 \times 10^{-8} \ll g_{cw}^{(3)}(0) \sim 3.6 \times 10^{-5} \ll g_{cw}^{(2)}(0) \sim 0.012 \ll 1$. Due to the tip-induced loss, $g_{cw}^{(2)}(0)$ is slightly larger than that in the ideal cavity. Such quantum backscattering-immune effect is different from the classical one.[51–57,59,60]

Specifically, the behavior of quantum correlation $g_{cw}^{(2)}(0)$ depends on both of χ and ϕ, while classical photon number N_{cw} is independent of the χ [Figure 2]. By fixing $\phi = \{0.21, 0.33\}\ \mu m$, the SPB can emerge with a specific strength of the nonlinearity, i.e., $\chi/\gamma = 0.5$. However, N_{cw} is still suppressed. In addition, by fixing $\phi = 0.27\ \mu m$, the quantum revival of SPB can only exist in the strong nonlinear regime ($\chi/\gamma > 1$), but cannot exist for $\chi/\gamma < 1$. In contrast, the classical revival of N_{cw} always exists with its maximum at the same position. Different from the classical optical devices against backscattering losses rely on nanotip-induced destructive interference,[51–54] such robust quantum effect relies on the interplay of the resonator nonlinearity and nanotip-induced optical coupling. This distinction may play the crucial role for designing robust quantum devices, where quantum fluctuations and correlations play a central role in the device performance.

The underlying physics can be understood from the interplay of the resonator nonlinearity and the tip-induced optical coupling by analyzing the photon-number probabilities and the transitions between different quantum states [Figure
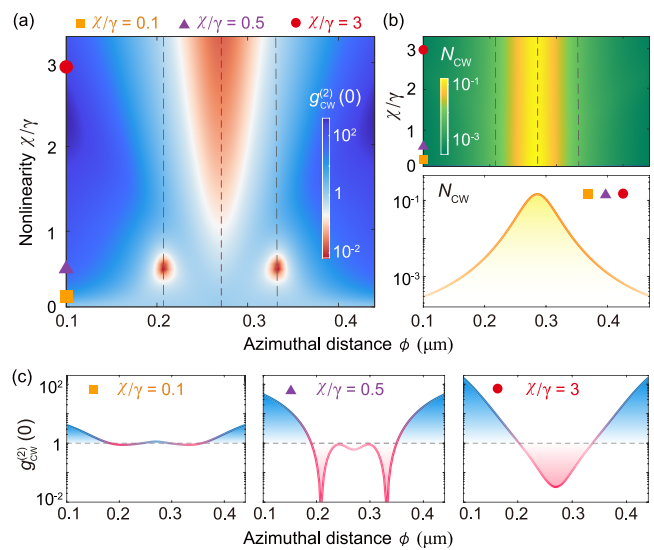

Figure 2. Robust quantum SPB effect is different from the behavior of classical N_{cw} by varying azimuthal distance ϕ and nonlinearity strengths χ/γ. (a) The quantum correlation of SPB, $g_{cw}^{(2)}(0) \ll 1$, can emerge at $\phi = \{0.21, 0.33\}\ \mu m$ (vertical gray dashed lines) for $\chi/\gamma = 0.5$ [purple triangles, the middle panel of (c)], while classical N_{cw} is still suppressed. Also, SPB cannot occur at $\phi = 0.27\ \mu m$ (vertical red dashed lines) for $\chi/\gamma < 1$ [orange squares, the left panel of (c)], but can occur for $\chi/\gamma > 1$ [red circles, the right panel of (c)]. (b) Meanwhile the classical N_{cw} always recovers to its maximum at $\phi = 0.27\ \mu m$. The other parameters are the same as those in Figure 1.

3], which is different from that in previous studies in classical optics,[51–57,59,60] i.e., merely relies on the scatterer-induced destructive interference, and focuses on light amplitudes.

We study the photon-number probabilities via the quantum trajectory method.[110] Our effective Hamiltonian is $\hat{H}_{eff} = \hat{H}_r - i\sum_{j=1,2}(\gamma/2)\hat{a}_j^\dagger \hat{a}_j$. For $\xi \ll \gamma$, by truncating the Hilbert space to $N = m + n = 3$, the states are $|\psi(t)\rangle = \sum_{m=0}^3 \sum_{n=0}^m C_{mn}|m, n\rangle$, where C_{mn} are probability amplitudes corresponding to $|m, n\rangle$. The probability of finding m photons in the CW mode and n photons in the CCW mode is given by $P_{mn} = |C_{mn}|^2$, which can also be obtained from the steady-state solutions ρ_{ss} of eq 4 via $P_{mn} = \langle m, n|\rho_{ss}|m, n\rangle$. An excellent agreement between our analytical results and numerical results is seen in Figure 3. Note that the effect of quantum jumps is ignored (considered) in the semiclassical analytical (quantum master equation) approach.[111]

For $\Delta = 0$, the input light can be resonant with the transitions from the vacuum to $|2, 0\rangle$ in the weak nonlinear regime ($\chi/\gamma < 1$). The corresponding probability amplitude can be obtained by solving the Schrödinger equation $i|\dot{\psi}(t)\rangle = \hat{H}_{eff}|\psi(t)\rangle$:

$$C_{20} = \frac{2\sqrt{2}\,\xi^2(\Delta_1\Delta_2 + 4|J|^2\chi/\Delta_2)}{\eta_1\eta_2} \qquad (5)$$

where $\Delta_1 = 2\Delta - i\gamma$, $\Delta_2 = \Delta_1 + 2\chi$, $\eta_1 = 4|J|^2 - \Delta_1^2$, and $\eta_2 = 4|J|^2 - \Delta_2^2$. However, SPB can occur with $P_{20} = 0$,[112–114] which can be understood from the destructive interference of two transition paths [Figure 3(a)]: $|1, 0\rangle \xrightarrow{\omega_L} |2, 0\rangle$ (blue), and $|1, 0\rangle \xrightarrow{J} |0, 1\rangle \xrightarrow{\omega_L} |1, 1\rangle \xrightarrow{J} |2, 0\rangle$ (green). By setting $C_{20} = 0$, the conditions of SPB are given by $\chi/\gamma = 0.5$, and $|J|/\gamma = 1$. For $J_0 = 1.8\gamma_1$, we have $r = 0.35\ \mu m$, and $\phi = \{0.21, 0.33\}\ \mu m$ [the inset in Figure 3(b)]. In contrast, N_{cw} cannot be totally revived
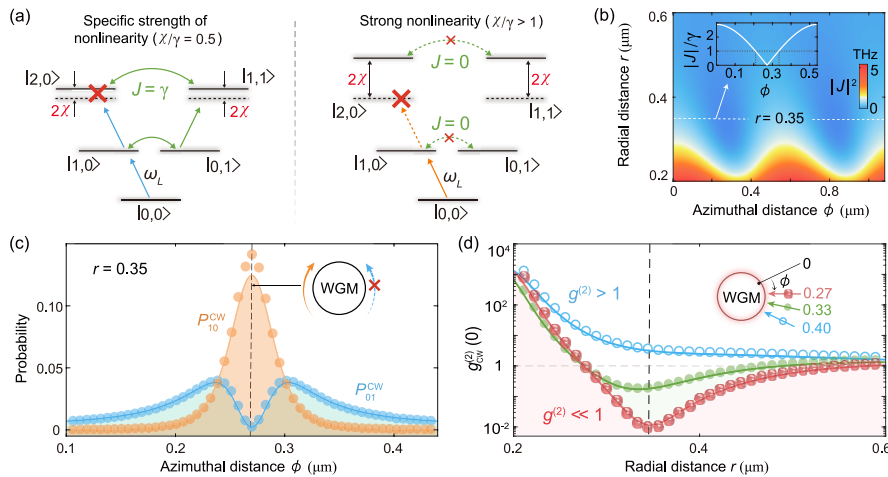
Figure 3. Physical mechanism of SPB can be understood from (a) the eigenenergy structures and transition paths, as well as (b) the nanotip-induced optical coupling. Specifically, for $\chi/\gamma = 0.5$ [left panel in (a)], optical coupling with $|J| = \gamma$ can be achieved at $\phi = \{0.21, 0.33\}$ μm and $r = 0.35$ μm [the inset of (b)]. SPB occurs because of the destructive interference of two transition paths (blue and green arrows) to state $|2, 0\rangle$. For $\chi/\gamma > 1$ [right panel in (b)], two optical modes decoupled ($J = 0$) at $\phi = 0.27$ μm and $r = 0.35$ μm. SPB emerges due to the unequal eigenenergy spaces. Such SPB effect can also be recognized via (c) the single-photon probability distribution and (d) second-order quantum correlation. In (c, d), the curves and markers correspond to the numerical and analytical results, respectively. The Kerr nonlinearity and other parameters are the same as those in Figure 1.

at the same positions due to the nonzero coupling ($J \neq 0$) between the CW and CCW modes.

The single-photon probabilities are given by

$$P_{10}^{\text{cw}} = 4\xi^2 \left| \frac{\Delta_1}{\eta_1} \right|^2, \quad P_{01}^{\text{ccw}} = 16\xi^2 \left| \frac{J}{\eta_1} \right|^2 \tag{6}$$

where P_{01}^{ccw} tends to be zero, and P_{10}^{cw} reaches its maximum for $J = 0$ [Figure 3(c)], i.e., $r = \ln(a_t/J_0)/2\alpha_v$ and $\phi = [(2l + 1)\pi - \theta - \theta_r r]/2k_{\text{opt}}$ with integer l. For $l = \{0, 1\}$, we have $\phi = \{0.27, 0.82\}$ μm [Figure 3(b)]. SPB emerges because the transition $|0, 0\rangle \rightarrow |1, 0\rangle$ is resonantly driven by the input light, but the transition $|1, 0\rangle \rightarrow |2, 0\rangle$ is detuned by 2χ, and the transitions between $|1, 0\rangle$ and $|0, 1\rangle$ are eliminated [Figure 3(a), right panel]. Such effect can be understood from the interplay of the strong nonlinearity induced unequal eigenenergy spaces ($\chi/\gamma > 1$), and the tip-induced vanishing of the coupling ($J = 0$). In contrast, the classical revival of N_{cw} merely relies on the condition of $J = 0$, regardless of χ.

The second-order quantum correlation is given by

$$g_{\text{cw}}^{(2)}(0) \simeq \frac{2P_{20}}{P_{10}^2} = \left| \frac{\eta_1(\Delta_1\Delta_2 + 4|J|^2\chi/\Delta_2)}{\Delta_1^2\eta_2} \right|^2 \tag{7}$$

With $J = 0$, we obtain $g_{\text{cw}}^{(2)}(0) \simeq [4(\chi/\gamma)^2 + 1]^{-1} < 1$, for $\chi > \gamma$ and $\Delta = 0$, which indicates SPB [Figure 3(d)]. When the tip is away from the cavity ($r > 0.6$ μm), the system behaves as a nonideal cavity without the tip and SPB cannot be observed. When the tip is close to the cavity ($0 < r < 0.2$ μm), increased γ and J enable the input light to be in resonance with higher photon-number states, resulting in photon bunching.[17]

To characterize the SPB against backscattering loss efficiency, we introduce a ratio by comparing the minimum of $g_{\text{cw}}^{(2)}(0)$ in our device ($J_0 \neq 0$) with that in an ideal cavity ($J_0 = 0$) under the same optical nonlinearities and driving fields:

$$\mathcal{R} = \max[0, \zeta], \quad \zeta \equiv \frac{1 - \min[g_{\text{cw}}^{(2)}(0)(J_0 \neq 0)]}{1 - \min[g_{\text{cw}}^{(2)}(0)(J_0 = 0)]} \tag{8}$$

Here, the quantity of $1 - \min[g_{\text{cw}}^{(2)}(0)]$ is the purity of the generated single photons, and $\mathcal{R} = 100\%$ denotes perfect backscattering immunity, indicating that the single photons generated in our system with the intrinsic backscattering have the same purity as those in the ideal case. Figure 4(a) shows
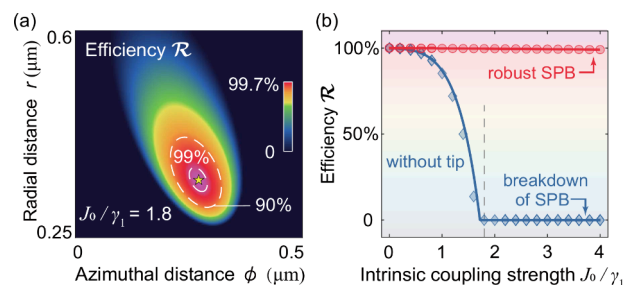

Figure 4. Robust SPB for different backscattering strengths. (a) SPB against backscattering loss efficiency $\mathcal{R}$ versus r and ϕ for $J_0/\gamma_1 = 1.8$ and $\Delta = 0$. (b) Efficiency $\mathcal{R}$ as a function of J_0 with (red) and without (blue) the nanotip, where the curves and markers show our numerical and analytical results, respectively. The Kerr nonlinearity and other parameters are the same as those in Figure 1.

that the efficiency $\mathcal{R}$ can reach 99.7% with $J_0/\gamma_1 = 1.8$ by adjusting the nanotip position at $r = 0.35$ μm and $\phi = 0.27$ μm. Furthermore, for the nonideal cavity without nanotip, such efficiency $\mathcal{R}$ gradually decreases with increasing J_0, and becomes 0 for $J_0/\gamma_1 = 1.8$ [Figure 4(b)], i.e., SPB is suppressed by the backscattering. However, robust SPB can exist with different backscattering strengths by introducing an additional tip with strong nonlinearities, which can be beneficial for protecting the generation or transmission of single photons, and improving the performance in realistic quantum devices.

We studied SPB against backscattering loss in a nonideal Kerr WGM cavity with a nanotip. The efficiency of such effect is up to 99.7% by tuning tip positions, which is robust with different backscattering strengths. More interestingly, we found that the behavior of this quantum effect is distinct from that of the classical mean-photon number with different strengths of

the nonlinearity, due to the interplay of the resonator nonlinearity and the tip-induced optical coupling.

This underlying principle can be extended to other types of platforms, e.g., optical parametric amplifiers or cavity QED systems, for exploring squeezing or entanglement against backscattering loss, and for generating robust Schrödinger cat states. It is also expected to explore multiphoton bundles against backscattering loss[115−117] or mutual blockade[15] and robust microwave-optical photon pair[118] by studying higher-order correlations. Our work provides a novel perspective toward enhancing the performance of quantum devices, opening a new way to protect or engineer fragile quantum resources, and holding the potential for implementations in quantum technologies, such as robust single-photon routing[119] in quantum communications or more robust quantum sensing.[120−122]

◼ AUTHOR INFORMATION

Corresponding Authors

Ran Huang − *Quantum Information Physics Theory Research Team, Quantum Computing Center, RIKEN, Wako-shi, Saitama 351-0198, Japan;* ◉ orcid.org/0000-0003-3850-9403; Email: ran.huang@riken.jp

Hui Jing − *Key Laboratory of Low-Dimensional Quantum Structures and Quantum Control of Ministry of Education, Department of Physics and Synergetic Innovation Center for Quantum Effects and Applications, Hunan Normal University, Changsha 410081, China; Institute for Quantum Science and Technology, College of Science, National University of Defense Technology, Changsha 410073, P.R.China;* ◉ orcid.org/0000-0001-5091-2057; Email: jinghui73@foxmail.com

Authors

Jian Tang − *Key Laboratory of Low-Dimensional Quantum Structures and Quantum Control of Ministry of Education, Department of Physics and Synergetic Innovation Center for Quantum Effects and Applications, Hunan Normal University, Changsha 410081, China*

Yunlan Zuo − *School of Physics and Chemistry, Hunan First Normal University, Changsha 410205, China; Key Laboratory of Low-Dimensional Quantum Structures and Quantum Control of Ministry of Education, Department of Physics and Synergetic Innovation Center for Quantum Effects and Applications, Hunan Normal University, Changsha 410081, China*

Xun-Wei Xu − *Key Laboratory of Low-Dimensional Quantum Structures and Quantum Control of Ministry of Education, Department of Physics and Synergetic Innovation Center for Quantum Effects and Applications, Hunan Normal University, Changsha 410081, China*

Adam Miranowicz − *Quantum Information Physics Theory Research Team, Quantum Computing Center, RIKEN, Wako-shi, Saitama 351-0198, Japan; Institute of Spintronics and Quantum Information, Faculty of Physics and Astronomy, Adam Mickiewicz University, 61-614 Poznań, Poland*

Franco Nori − *Quantum Information Physics Theory Research Team, Quantum Computing Center, RIKEN, Wako-shi, Saitama 351-0198, Japan; Physics Department, The University of Michigan, Ann Arbor, Michigan 48109-1040, United States;* ◉ orcid.org/0000-0003-3682-7432

Complete contact information is available at:

◼ REFERENCES

(1) Fürst, J. U.; Strekalov, D. V.; Elser, D.; Aiello, A.; Andersen, U. L.; Marquardt, C.; Leuchs, G. Quantum Light from a Whispering-Gallery-Mode Disk Resonator. *Phys. Rev. Lett.* **2011**, *106*, No. 113901.

(2) Lu, X.; Li, Q.; Westly, D. A.; Moille, G.; Singh, A.; Anant, V.; Srinivasan, K. Chip-integrated visible-telecom entangled photon pair source for quantum communication. *Nat. Phys.* **2019**, *15*, 373.

(3) Brooks, A.; Chu, X.-L.; Liu, Z.; Schott, R.; Ludwig, A.; Wieck, A. D.; Midolo, L.; Lodahl, P.; Rotenberg, N. Integrated Whispering-Gallery-Mode Resonator for Solid-State Coherent Quantum Photonics. *Nano Lett.* **2021**, *21*, 8707.

(4) Knill, E.; Laflamme, R.; Milburn, G. J. A scheme for efficient quantum computation with linear optics. *Nature (London)* **2001**, *409*, 46.

(5) Kok, P.; Munro, W. J.; Nemoto, K.; Ralph, T. C.; Dowling, J. P.; Milburn, G. J. Linear optical quantum computing with photonic qubits. *Rev. Mod. Phys.* **2007**, *79*, 135.

(6) O'Brien, J. L. Optical Quantum Computing. *Science* **2007**, *318*, 1567.

(7) O'brien, J. L.; Furusawa, A.; Vučković, J. Photonic quantum technologies. *Nat. Photonnics* **2009**, *3*, 687.

(8) Dowling, J. P. Quantum optical metrology − the lowdown on high-N00N states. *Contemp. Phys.* **2008**, *49*, 125.

(9) Tian, L.; Carmichael, H. J. Quantum trajectory simulations of two-state behavior in an optical cavity containing one atom. *Phys. Rev. A* **1992**, *46*, No. R6801.

(10) Leoński, W.; Tanaś, R. Possibility of producing the one-photon state in a kicked cavity with a nonlinear Kerr medium. *Phys. Rev. A* **1994**, *49*, R20.

(11) Miranowicz, A.; Leoński, W.; Dyrting, S.; Tanaś, R. Quantum state engineering in finite-dimensional Hilbert space. *Acta Phys. Slovaca* **1996**, *46*, 451.

(12) Imamoḡlu, A.; Schmidt, H.; Woods, G.; Deutsch, M. Strongly Interacting Photons in a Nonlinear Cavity. *Phys. Rev. Lett.* **1997**, *79*, 1467.

(13) Birnbaum, K. M.; Boca, A.; Miller, R.; Boozer, A. D.; Northup, T. E.; Kimble, H. J. Photon blockade in an optical cavity with one trapped atom. *Nature (London)* **2005**, *436*, 87.

(14) Dayan, B.; Parkins, A. S.; Aoki, T.; Ostby, E. P.; Vahala, K. J.; Kimble, H. J. A Photon Turnstile Dynamically Regulated by One Atom. *Science* **2008**, *319*, 1062.

(15) Hamsen, C.; Tolazzi, K. N.; Wilk, T.; Rempe, G. Strong coupling between photons of two light fields mediated by one atom. *Nat. Phys.* **2018**, *14*, 885.

(16) Hennessy, K.; Badolato, A.; Winger, M.; Gerace, D.; Atatüre, M.; Gulde, S.; Fält, S.; Hu, E. L.; Imamoğlu, A. Quantum nature of a strongly coupled single quantum dot-cavity system. *Nature (London)* **2007**, *445*, 896.

(17) Faraon, A.; Fushman, I.; Englund, D.; Stoltz, N.; Petroff, P.; Vučković, J. Coherent generation of non-classical light on a chip via photon-induced tunnelling and blockade. *Nat. Phys.* **2008**, *4*, 859.

(18) Reinhard, A.; Volz, T.; Winger, M.; Badolato, A.; Hennessy, K. J.; Hu, E. L.; Imamoğlu, A. Strongly correlated photons on a chip. *Nat. Photonics* **2012**, *6*, 93.

(19) Müller, K.; Rundquist, A.; Fischer, K. A.; Sarmiento, T.; Lagoudakis, K. G.; Kelaita, Y. A.; Sánchez Muñoz, C.; del Valle, E.; Laussy, F. P.; Vučković, J. Coherent Generation of Nonclassical Light on Chip via Detuned Photon Blockade. *Phys. Rev. Lett.* **2015**, *114*, No. 233601.

(20) Snijders, H. J.; Frey, J. A.; Norman, J.; Flayac, H.; Savona, V.; Gossard, A. C.; Bowers, J. E.; van Exter, M. P.; Bouwmeester, D.; Löffler, W. Observation of the Unconventional Photon Blockade. *Phys. Rev. Lett.* **2018**, *121*, No. 043601.

(21) Lang, C.; Bozyigit, D.; Eichler, C.; Steffen, L.; Fink, J. M.; Abdumalikov, A. A.; Baur, M.; Filipp, S.; da Silva, M. P.; Blais, A.; Wallraff, A. Observation of Resonant Photon Blockade at Microwave Frequencies Using Correlation Function Measurements. *Phys. Rev. Lett.* **2011**, *106*, No. 243601.

(22) Hoffman, A. J.; Srinivasan, S. J.; Schmidt, S.; Spietz, L.; Aumentado, J.; Türeci, H. E.; Houck, A. A. Dispersive Photon Blockade in a Superconducting Circuit. *Phys. Rev. Lett.* **2011**, *107*, No. 053602.

(23) Vaneph, C.; Morvan, A.; Aiello, G.; Féchant, M.; Aprili, M.; Gabelli, J.; Estève, J. Observation of the Unconventional Photon Blockade in the Microwave Domain. *Phys. Rev. Lett.* **2018**, *121*, No. 043602.

(24) Rolland, C.; Peugeot, A.; Dambach, S.; Westig, M.; Kubala, B.; Mukharsky, Y.; Altimiras, C.; le Sueur, H.; Joyez, P.; Vion, D.; Roche, P.; Esteve, D.; Ankerhold, J.; Portier, F. Antibunched Photons Emitted by a dc-Biased Josephson Junction. *Phys. Rev. Lett.* **2019**, *122*, No. 186804.

(25) Collodo, M. C.; Potočnik, A.; Gasparinetti, S.; Besse, J.-C.; Pechal, M.; Sameti, M.; Hartmann, M. J.; Wallraff, A.; Eichler, C. Observation of the Crossover from Photon Ordering to Delocalization in Tunably Coupled Resonators. *Phys. Rev. Lett.* **2019**, *122*, No. 183601.

(26) Peyronel, T.; Firstenberg, O.; Liang, Q.-Y.; Hofferberth, S.; Gorshkov, A. V.; Pohl, T.; Lukin, M. D.; Vuletić, V. Quantum nonlinear optics with single photons enabled by strongly interacting atoms. *Nature (London)* **2012**, *488*, 57.

(27) Prasad, A. S.; Hinney, J.; Mahmoodian, S.; Hammerer, K.; Rind, S.; Schneeweiss, P.; Sørensen, A. S.; Volz, J.; Rauschenbeutel, A. Correlating photons using the collective nonlinear response of atoms weakly coupled to an optical mode. *Nat. Photonics* **2020**, *14*, 719.

(28) Fedorov, G. P.; Remizov, S. V.; Shapiro, D. S.; Pogosov, W. V.; Egorova, E.; Tsitsilin, I.; Andronik, M.; Dobronosova, A. A.; Rodionov, I. A.; Astafiev, O. V.; Ustinov, A. V. Photon Transport in a Bose-Hubbard Chain of Superconducting Artificial Atoms. *Phys. Rev. Lett.* **2021**, *126*, No. 180503.

(29) Hamsen, C.; Tolazzi, K. N.; Wilk, T.; Rempe, G. Two-Photon Blockade in an Atom-Driven Cavity QED System. *Phys. Rev. Lett.* **2017**, *118*, No. 133604.

(30) Chakram, S.; He, K.; Dixit, A. V.; Oriani, A. E.; Naik, R. K.; Leung, N.; Kwon, H.; Ma, W.-L.; Jiang, L.; Schuster, D. I. Multimode photon blockade. *Nat. Phys.* **2022**, *18*, 879.

(31) Chakram, S.; Oriani, A. E.; Naik, R. K.; Dixit, A. V.; He, K.; Agrawal, A.; Kwon, H.; Schuster, D. I. Seamless High-Q Microwave

Cavities for Multimode Circuit Quantum Electrodynamics. *Phys. Rev. Lett.* **2021**, *127*, No. 107701.

(32) Lin, G.; Coillet, A.; Chembo, Y. K. Nonlinear photonics with high-Q whispering-gallery-mode resonators. *Adv. Opt. Photon.* **2017**, *9*, 828.

(33) Strekalov, D. V.; Marquardt, C.; Matsko, A. B.; Schwefel, H. G. L.; Leuchs, G. Nonlinear and quantum optics with whispering gallery resonators. *J. Opt.* **2016**, *18*, No. 123002.

(34) Li, B.-B.; Clements, W. R.; Yu, X.-C.; Shi, K.; Gong, Q.; Xiao, Y.-F. Single nanoparticle detection using split-mode microcavity Raman lasers. *Proc. Natl. Acad. Sci. U. S. A.* **2014**, *111*, No. 14657.

(35) Tang, S.-J.; Zhang, M.; Sun, J.; Meng, J.-W.; Xiong, X.; Gong, Q.; Jin, D.; Yang, Q.-F.; Xiao, Y.-F. Single-particle photoacoustic vibrational spectroscopy using optical microresonators. *Nat. Photonics* **2023**, *17*, 951.

(36) Mao, W.; Li, Y.; Jiang, X.; Liu, Z.; Yang, L. A whispering-gallery scanning microprobe for Raman spectroscopy and imaging. *Light: Sci. Appl.* **2023**, *12*, 247.

(37) Yu, D.; Humar, M.; Meserve, K.; Bailey, R. C.; Chormaic, S. N.; Vollmer, F. Whispering-gallery-mode sensors for biological and physical sensing. *Nat. Rev. Methods Primers* **2021**, *1*, 83.

(38) Foreman, M. R.; Swaim, J. D.; Vollmer, F. Whispering gallery mode sensors. *Adv. Opt. Photon.* **2015**, *7*, 168.

(39) Yang, Q.-F.; Yi, X.; Yang, K. Y.; Vahala, K. Counter-propagating solitons in microresonators. *Nat. Photonics* **2017**, *11*, 560.

(40) Peng, B.; Özdemir, Ş. K.; Liertzer, M.; Chen, W.; Kramer, J.; Yılmaz, H.; Wiersig, J.; Rotter, S.; Yang, L. Chiral modes and directional lasing at exceptional points. *Proc. Natl. Acad. Sci. U.S.A.* **2016**, *113*, 6845.

(41) Ren, L.; Yuan, S.; Zhu, S.; Shi, L.; Zhang, X. Backscattering-Induced Chiral Absorption in Optical Microresonators. *ACS Photonics* **2023**, *10*, 3797.

(42) Wu, Z.; Wang, Z.; Meng, Y.; Chen, J.; Xi, X.; Shum, P. P.; Gao, Z. Realization of a Chiral Topological Whispering-Gallery-Mode Cavity in Gyromagnetic Photonic Crystals. *Laser & Photonics Reviews* **2024**, 2401451.

(43) Lu, X.; McClung, A.; Srinivasan, K. High-Q slow light and its localization in a photonic crystal microring. *Nat. Photonics* **2022**, *16*, 66.

(44) Suh, M.-G.; Yang, Q.-F.; Yang, K. Y.; Yi, X.; Vahala, K. J. Microresonator soliton dual-comb spectroscopy. *Science* **2016**, *354*, 600.

(45) Griffith, A. G.; Lau, R. K. W.; Cardenas, J.; Okawachi, Y.; Mohanty, A.; Fain, R.; Lee, Y. H. D.; Yu, M.; Phare, C. T.; Poitras, C. B.; Gaeta, A. L.; Lipson, M. Silicon-chip mid-infrared frequency comb generation. *Nat. Commun.* **2015**, *6*, 6299.

(46) Cutler, C. C.; Newton, S. A.; Shaw, H. J. Limitation of rotation sensing by scattering. *Opt. Lett.* **1980**, *5*, 488.

(47) Lai, Y.-H.; Suh, M.-G.; Lu, Y.-K.; Shen, B.; Yang, Q.-F.; Wang, H.; Li, J.; Lee, S. H.; Yang, K. Y.; Vahala, K. Earth rotation measured by a chip-scale ring laser gyroscope. *Nat. Photonics* **2020**, *14*, 345.

(48) Liang, W.; Ilchenko, V. S.; Savchenkov, A. A.; Dale, E.; Eliyahu, D.; Matsko, A. B.; Maleki, L. Resonant microphotonic gyroscope. *Optica* **2017**, *4*, 114.

(49) Patel, K. A.; Dynes, J. F.; Choi, I.; Sharpe, A. W.; Dixon, A. R.; Yuan, Z. L.; Penty, R. V.; Shields, A. J. Coexistence of High-Bit-Rate Quantum Key Distribution and Data on Optical Fiber. *Phys. Rev. X* **2012**, *2*, No. 041010.

(50) Subacius, D.; Zavriyev, A.; Trifonov, A. Backscattering limitation for fiber-optic quantum key distribution systems. *Appl. Phys. Lett.* **2005**, *86*, No. 011103.

(51) Li, A.; Bogaerts, W. Fundamental suppression of backscattering in silicon microrings. *Opt. Express* **2017**, *25*, 2092.

(52) Jaffe, M.; Palm, L.; Baum, C.; Taneja, L.; Kumar, A.; Simon, J. Understanding and suppressing backscatter in optical resonators. *Optica* **2022**, *9*, 878.

(53) Lee, H.; Kecebas, A.; Wang, F.; Chang, L.; Özdemir, Ş. K.; Gu, T. Chiral exceptional point and coherent suppression of back-

scattering in silicon microring with low loss Mie scatterer. *eLight* **2023**, *3*, 20.

(54) Svela, A. Ø.; Silver, J. M.; Del Bino, L.; Zhang, S.; Woodley, M. T. M.; Vanner, M. R.; Del'Haye, P. Coherent suppression of backscattering in optical microresonators. *Light: Sci. Appl.* **2020**, *9*, 204.

(55) Kim, S.; Taylor, J. M.; Bahl, G. Dynamic suppression of Rayleigh backscattering in dielectric resonators. *Optica* **2019**, *6*, 1016.

(56) Örsel, O. E.; Noh, J.; Bahl, G. Electrically-controlled suppression of Rayleigh backscattering in an integrated photonic circuit. *Nanophotonics* **2024**, *13*, 173.

(57) Krenz, G.; Bux, S.; Slama, S.; Zimmermann, C.; Courteille, P. W. Controlling mode locking in optical ring cavities. *Appl. Phys. B: Laser Opt.* **2007**, *87*, 643.

(58) Zhang, P.-J.; Ji, Q.-X.; Cao, Q.-T.; Wang, H.; Liu, W.; Gong, Q.; Xiao, Y.-F. Single-mode characteristic of a supermode microcavity Raman laser. *Proc. Natl. Acad. Sci. U. S. A.* **2021**, *118*, No. e2101605118.

(59) Chen, Y.; Zhang, Y.-L.; Shen, Z.; Zou, C.-L.; Guo, G.-C.; Dong, C.-H. Synthetic Gauge Fields in a Single Optomechanical Resonator. *Phys. Rev. Lett.* **2021**, *126*, No. 123603.

(60) Jiang, X.; Yin, S.; Li, H.; Quan, J.; Goh, H.; Cotrufo, M.; Kullig, J.; Wiersig, J.; Alù, A. Coherent control of chaotic optical microcavity with reflectionless scattering modes. *Nat. Phys.* **2024**, *20*, 109.

(61) Jiao, Y.-F.; Zhang, S.-D.; Zhang, Y.-L.; Miranowicz, A.; Kuang, L.-M.; Jing, H. Nonreciprocal Optomechanical Entanglement against Backscattering Losses. *Phys. Rev. Lett.* **2020**, *125*, No. 143605.

(62) Liu, J.-X.; Jiao, Y.-F.; Li, Y.; Xu, X.-W.; He, Q.-Y.; Jing, H. Phase-controlled asymmetric optomechanical entanglement against optical backscattering. *Sci. China Phys. Mech. Astron.* **2023**, *66*, No. 230312.

(63) Dong, M.-X.; Xia, K.-Y.; Zhang, W.-H.; Yu, Y.-C.; Ye, Y.-H.; Li, E.-Z.; Zeng, L.; Ding, D.-S.; Shi, B.-S.; Guo, G.-C.; Nori, F. All-optical reversible single-photon isolation at room temperature. *Sci. Adv.* **2021**, *7*, No. eabe8924.

(64) Yan, C.-H.; Li, M.; Xu, X.-B.; Zhang, Y.-L.; Ma, X.-Y.; Zou, C.-L. Unidirectional propagation of single photons realized by a scatterer coupled to whispering-gallery-mode microresonators. *Phys. Rev. A* **2023**, *107*, No. 033713.

(65) Matres, J.; Sorin, W. V. Simple model for ring resonators backscatter. *Opt. Express* **2017**, *25*, 3242.

(66) Wiersig, J. Structure of whispering-gallery modes in optical microdisks perturbed by nanoparticles. *Phys. Rev. A* **2011**, *84*, No. 063828.

(67) Mohageg, M.; Savchenkov, A.; Maleki, L. Coherent back-scattering in lithium niobate whispering-gallery-mode resonators. *Opt. Lett.* **2007**, *32*, 2574.

(68) Li, A.; Van Vaerenbergh, T.; De Heyn, P.; Bienstman, P.; Bogaerts, W. Backscattering in silicon microring resonators: a quantitative analysis. *Laser Photonics Rev.* **2016**, *10*, 420.

(69) Borselli, M.; Johnson, T. J.; Painter, O. Beyond the Rayleigh scattering limit in high-Q silicon microdisks: theory and experiment. *Opt. Express* **2005**, *13*, 1515−1530.

(70) Srinivasan, K.; Painter, O. Mode coupling and cavity-quantum-dot interactions in a fiber-coupled microdisk cavity. *Phys. Rev. A* **2007**, *75*, No. 023814.

(71) Srinivasan, K.; Painter, O. Linear and nonlinear optical spectroscopy of a strongly coupled microdisk-quantum dot system. *Nature (London)* **2007**, *450*, 862−865.

(72) Wiersig, J. Enhancing the Sensitivity of Frequency and Energy Splitting Detection by Using Exceptional Points: Application to Microcavity Sensors for Single-Particle Detection. *Phys. Rev. Lett.* **2014**, *112*, No. 203901.

(73) Huang, R.; Özdemir, Ş. K.; Liao, J.-Q.; Minganti, F.; Kuang, L.-M.; Nori, F.; Jing, H. Exceptional Photon Blockade: Engineering Photon Blockade with Chiral Exceptional Points. *Laser Photonics Rev.* **2022**, *16*, No. 2100430.

(74) Chen, W.; Kaya Özdemir, Ş.; Zhao, G.; Wiersig, J.; Yang, L. Exceptional points enhance sensing in an optical microcavity. *Nature (London)* **2017**, *548*, 192.

(75) Mazzei, A.; Götzinger, S.; de S. Menezes, L.; Zumofen, G.; Benson, O.; Sandoghdar, V. Controlled Coupling of Counter-propagating Whispering-Gallery Modes by a Single Rayleigh Scatterer: A Classical Problem in a Quantum Optical Light. *Phys. Rev. Lett.* **2007**, *99*, No. 173603.

(76) Xu, Y.; Tang, S.-J.; Yu, X.-C.; Chen, Y.-L.; Yang, D.; Gong, Q.; Xiao, Y.-F. Mode splitting induced by an arbitrarily shaped Rayleigh scatterer in a whispering-gallery microcavity. *Phys. Rev. A* **2018**, *97*, No. 063828.

(77) Miranowicz, A.; Paprzycka, M.; Liu, Y.-x.; Bajer, J.; Nori, F. Two-photon and three-photon blockades in driven nonlinear systems. *Phys. Rev. A* **2013**, *87*, No. 023809.

(78) Schmidt, H.; Imamoḡlu, A. Giant Kerr nonlinearities obtained by electromagnetically induced transparency. *Opt. Lett.* **1996**, *21*, 1936.

(79) Kirchmair, G.; Vlastakis, B.; Leghtas, Z.; Nigg, S. E.; Paik, H.; Ginossar, E.; Mirrahimi, M.; Frunzio, L.; Girvin, S. M.; Schoelkopf, R. J. Observation of quantum state collapse and revival due to the single-photon Kerr effect. *Nature (London)* **2013**, *495*, 205.

(80) Wang, Y.-P.; Zhang, G.-Q.; Zhang, D.; Li, T.-F.; Hu, C.-M.; You, J. Q. Bistability of Cavity Magnon Polaritons. *Phys. Rev. Lett.* **2018**, *120*, No. 057202.

(81) Rabl, P. Photon Blockade Effect in Optomechanical Systems. *Phys. Rev. Lett.* **2011**, *107*, No. 063601.

(82) Nunnenkamp, A.; Børkje, K.; Girvin, S. M. Single-Photon Optomechanics. *Phys. Rev. Lett.* **2011**, *107*, No. 063602.

(83) Liao, J.-Q.; Nori, F. Photon blockade in quadratically coupled optomechanical systems. *Phys. Rev. A* **2013**, *88*, No. 023853.

(84) Gong, Z. R.; Ian, H.; Liu, Y.-x.; Sun, C. P.; Nori, F. Effective Hamiltonian approach to the Kerr nonlinearity in an optomechanical system. *Phys. Rev. A* **2009**, *80*, No. 065801.

(85) Marin-Palomo, P.; Kemal, J. N.; Karpov, M.; Kordts, A.; Pfeifle, J.; Pfeiffer, M. H. P.; Trocha, P.; Wolf, S.; Brasch, V.; Anderson, M. H.; Rosenberger, R.; Vijayan, K.; Freude, W.; Kippenberg, T. J.; Koos, C. Microresonator-based solitons for massively parallel coherent optical communications. *Nature (London)* **2017**, *546*, 274.

(86) Cao, Q.-T.; Wang, H.; Dong, C.-H.; Jing, H.; Liu, R.-S.; Chen, X.; Ge, L.; Gong, Q.; Xiao, Y.-F. Experimental Demonstration of Spontaneous Chirality in a Nonlinear Microresonator. *Phys. Rev. Lett.* **2017**, *118*, No. 033901.

(87) Hales, J. M.; Chi, S.-H.; Allen, T.; Benis, S.; Munera, N.; Perry, J. W.; McMorrow, D.; Hagan, D. J.; Stryland, E. W. V. Third-Order Nonlinear Optical Coefficients of Si and GaAs in the Near-Infrared Spectral Region. *Conference on Lasers and Electro-Optics* **2018**, JTu2A.59.

(88) Heuck, M.; Jacobs, K.; Englund, D. R. Controlled-Phase Gate Using Dynamically Coupled Cavities and Optical Nonlinearities. *Phys. Rev. Lett.* **2020**, *124*, No. 160501.

(89) Choi, H.; Heuck, M.; Englund, D. Self-Similar Nanocavity Design with Ultrasmall Mode Volume for Single-Photon Non-linearities. *Phys. Rev. Lett.* **2017**, *118*, No. 223605.

(90) Boyd, R. W. *Nonlinear Optics*, 3rd ed.; Academic Press: Burlington, 2008.

(91) Ferretti, S.; Gerace, D. Single-photon nonlinear optics with Kerr-type nanostructured materials. *Phys. Rev. B* **2012**, *85*, No. 033303.

(92) Eckardt, A.; Hauke, P.; Soltan-Panahi, P.; Becker, C.; Sengstock, K.; Lewenstein, M. Frustrated quantum antiferromagnetism with ultracold bosons in a triangular lattice. *Europhys. Lett.* **2010**, *89*, No. 10010.

(93) Glauber, R. J. The Quantum Theory of Optical Coherence. *Phys. Rev.* **1963**, *130*, 2529.

(94) Scully, M. O.; Zubairy, M. S. *Quantum Optics*; Cambridge University Press: Cambridge, England, 1997.

(95) Agarwal, G. S. *Quantum Optics*; Cambridge University Press: Cambridge, England, 2012.

(96) Johansson, J.; Nation, P.; Nori, F. QuTiP: An open-source Python framework for the dynamics of open quantum systems. *Comput. Phys. Commun.* **2012**, *183*, 1760.

(97) Johansson, J.; Nation, P.; Nori, F. QuTiP 2: A Python framework for the dynamics of open quantum systems. *Comput. Phys. Commun.* **2013**, *184*, 1234.

(98) Vahala, K. J. Optical microcavities. *Nature (London)* **2003**, *424*, 839.

(99) Spillane, S. M.; Kippenberg, T. J.; Vahala, K. J.; Goh, K. W.; Wilcut, E.; Kimble, H. J. Ultrahigh-*Q* toroidal microresonators for cavity quantum electrodynamics. *Phys. Rev. A* **2005**, *71*, No. 013817.

(100) Pavlov, N. G.; Lihachev, G.; Koptyaev, S.; Lucas, E.; Karpov, M.; Kondratiev, N. M.; Bilenko, I. A.; Kippenberg, T. J.; Gorodetsky, M. L. Soliton dual frequency combs in crystalline microresonators. *Opt. Lett.* **2017**, *42*, 514.

(101) Huet, V.; Rasoloniaina, A.; Guillemé, P.; Rochard, P.; Féron, P.; Mortier, M.; Levenson, A.; Bencheikh, K.; Yacomotti, A.; Dumeige, Y. Millisecond Photon Lifetime in a Slow-Light Micro-cavity. *Phys. Rev. Lett.* **2016**, *116*, No. 133902.

(102) Jin, W.; Yang, Q.-F.; Chang, L.; Shen, B.; Wang, H.; Leal, M. A.; Wu, L.; Gao, M.; Feshali, A.; Paniccia, M.; Vahala, K. J.; Bowers, J. E. Hertz-linewidth semiconductor lasers using CMOS-ready ultra-high-*Q* microresonators. *Nat. Photonnics* **2021**, *15*, 346.

(103) Del'Haye, P.; Diddams, S. A.; Papp, S. B. Laser-machined ultra-high-Q microrod resonators for nonlinear optics. *Appl. Phys. Lett.* **2013**, *102*, No. 221119.

(104) Alam, M. Z.; De Leon, I.; Boyd, R. W. Large optical nonlinearity of indium tin oxide in its epsilon-near-zero region. *Science* **2016**, *352*, 795.

(105) Zielińska, J. A.; Mitchell, M. W. Self-tuning optical resonator. *Opt. Lett.* **2017**, *42*, 5298.

(106) Wang, X.; Korzh, B. A.; Weigel, P. O.; Nemchick, D. J.; Drouin, B. J.; Becker, W.; Zhao, Q.-Y.; Zhu, D.; Colangelo, M.; Dane, A. E.; Berggren, K. K.; Shaw, M. D.; Mookherjea, S. Oscilloscopic Capture of Greater-Than-100 GHz, Ultra-Low Power Optical Waveforms Enabled by Integrated Electrooptic Devices. *J. Lightwave Technol.* **2020**, *38*, 166.

(107) Svela, A. Ø. Near-field-scattering-based Optical Control and Brillouin Optomechanics in Optical Microresonators. Ph.D. thesis, Imperial College London, 2022.

(108) Hagart-Alexander, C. In *Instrumentation Reference Book*, 4th ed.; Boyes, W., Ed.; Butterworth-Heinemann: Boston, 2010; pp 269–326.

(109) Karabchevsky, A.; Katiyi, A.; Ang, A. S.; Hazan, A. On-chip nanophotonics and future challenges. *Nanophotonics* **2020**, *9*, 3733.

(110) Plenio, M. B.; Knight, P. L. The quantum-jump approach to dissipative dynamics in quantum optics. *Rev. Mod. Phys.* **1998**, *70*, 101.

(111) Minganti, F.; Miranowicz, A.; Chhajlany, R. W.; Nori, F. Quantum exceptional points of non-Hermitian Hamiltonians and Liouvillians: The effects of quantum jumps. *Phys. Rev. A* **2019**, *100*, No. 062131.

(112) Liew, T. C. H.; Savona, V. Single Photons from Coupled Quantum Modes. *Phys. Rev. Lett.* **2010**, *104*, No. 183601.

(113) Bamba, M.; Imamoḡlu, A.; Carusotto, I.; Ciuti, C. Origin of strong photon antibunching in weakly nonlinear photonic molecules. *Phys. Rev. A* **2011**, *83*, No. 021802.

(114) Flayac, H.; Savona, V. Unconventional photon blockade. *Phys. Rev. A* **2017**, *96*, No. 053810.

(115) Muñoz, C. S.; Del Valle, E.; Tudela, A. G.; Müller, K.; Lichtmannecker, S.; Kaniber, M.; Tejedor, C.; Finley, J. J.; Laussy, F. P. Emitters of *N*-photon bundles. *Nat. Photonics* **2014**, *8*, 550.

(116) Bin, Q.; Lü, X.-Y.; Laussy, F. P.; Nori, F.; Wu, Y. *N*-Phonon Bundle Emission via the Stokes Process. *Phys. Rev. Lett.* **2020**, *124*, No. 053601.

(117) Bin, Q.; Wu, Y.; Lü, X.-Y. Parity-Symmetry-Protected Multiphoton Bundle Emission. *Phys. Rev. Lett.* **2021**, *127*, No. 073602.

(118) Meesala, S.; Wood, S.; Lake, D.; Chiappina, P.; Zhong, C.; Beyer, A. D.; Shaw, M. D.; Jiang, L.; Painter, O. Non-classical microwave−optical photon pair generation with a chip-scale trans-ducer. *Nat. Phys.* **2024**, *20*, 871.

(119) Aoki, T.; Parkins, A. S.; Alton, D. J.; Regal, C. A.; Dayan, B.; Ostby, E.; Vahala, K. J.; Kimble, H. J. Efficient Routing of Single Photons by One Atom and a Microtoroidal Cavity. *Phys. Rev. Lett.* **2009**, *102*, No. 083601.

(120) Fleury, R.; Sounas, D.; Alù, A. An invisible acoustic sensor based on parity-time symmetry. *Nat. Commun.* **2015**, *6*, 5905.

(121) Yang, T.; Bai, X.; Gao, D.; Wu, L.; Li, B.; Thong, J. T. L.; Qiu, C.-W. Invisible Sensors: Simultaneous Sensing and Camouflaging in Multiphysical Fields. *Adv. Mater.* **2015**, *27*, 7752.

(122) Xu, J.; Mao, Y.; Li, Z.; Zuo, Y.; Zhang, J.; Yang, B.; Xu, W.; Liu, N.; Deng, Z.-J.; Chen, W.; Xia, K.; Qiu, C.-W.; Zhu, Z.; Jing, H.; Liu, K. Single-cavity loss-enabled nanometrology. *Nat. Nanotechnol.* **2024**, *19*, 1472−1477.